H_2^+ photodissociation by an intense pulsed photonic Fock state

Amit K. Paul,[1] Satrajit Adhikari,[1] Michael Baer,[2] and Roi Baer[3]

[1]*Department of Physical Chemistry, Indian Association for the Cultivation of Science, Jadavpur, Kolkata 700 032, India*

[2]*Fritz Haber Research Center for Molecular Dynamics, The Hebrew University of Jerusalem, Jerusalem 91904, Israel*

[3]*Fritz Haber Center for Molecular Dynamics, Institute of Chemistry, The Hebrew University of Jerusalem, Jerusalem 91904, Israel*

(Received 7 October 2009; published 25 January 2010)

We study the photodissociation of the H_2^+ molecule by ultrashort Fock-state electromagnetic pulses (EMPs). We use the Born-Oppenheimer treatment combined with an explicit photon number representation via diabatic electrophoton potential surfaces for simplification of the basic equations. We discuss the issue of the number of photon states required and show that six photon states enable good accuracy for photoproduct kinetic energies of up to 3 eV. We calculate photodissociation probabilities and nuclear kinetic-energy (KE) distributions of the photodissociation products for 800-nm, 50-TW/cm^2 pulses. We show that KE distributions depend on three pulse durations of 10, 20, and 45 fs and on various initial vibrational states of the molecule. We compare the Fock-state results to those obtained by "conventional," i.e., coherent-state, laser pulses of equivalent electric fields and durations. The effects of the quantum state of EMPs on the photodissociation dynamics are especially strong for high initial vibrational states of H_2^+. While coherent-state pulses suppress photodissociation for the high initial vibrational states of H_2^+, the Fock-state pulses enhance it.

DOI: 10.1103/PhysRevA.81.013412 PACS number(s): 33.80.Wz, 33.80.Eh

I. INTRODUCTION

The interaction of molecular systems and laser pulses has been drawing much attention for many years and has a variety of applications in atomic physics [1], molecular physics [2], laser cooling [3], laser technology [4], coherent control [5–9], and the study of basic quantum mechanics. Of these, ultrashort pulses of high intensity (>10 TW/cm^2), are of special interest [10–12]. These processes are invariably associated with a delicate interplay of electronic and nuclear dynamics, a topic forming the focus of numerous experimental [13–23] and theoretical studies [9,24–40].

Light produced in standard laser cavities is in a coherent state, which has several characteristics similar to a classical electromagnetic field. The coherent state is a specific linear combination of Fock states $|N\rangle$ (where N is the number of photons) having the minimal allowed uncertainty $\Delta N \Delta\phi = \frac{\hbar}{2}$ (where ϕ is the photon phase) [41]. The "semiclassical" treatment of a laser-molecule interaction relies on the fact that light is in a coherent state. This leads to a Schrödinger equation for the charges of the molecule which are affected only through the expectation value of the electric field $\vec{E}$. This approach forms the basis for almost all published treatments of strong laser-molecule interactions. The effects of the more exotic nonclassical, i.e., quantum, states of light on photochemistry and molecular spectroscopy is recently drawing increasing attention [42,43] as the techniques for controlling quantum electromagnetic states evolve [44–54].

The effect of deviations from light coherency on molecular dynamics has recently been studied theoretically in the case of the photodissociation dynamics of H_2^+ following a 600 nm, 100 TW/cm^2 pulse [55]. That study established the basic method and covered a limited amount of results. This paper presents more detailed results concerning the comparison of coherent and Fock-state calculations and their dependence on pulse width and on the initial quantum state of the molecule. We first review the theory (Sec. II) and then use a 790 nm, 50 TW/cm^2 pulse to study the convergence properties of the calculations with respect to the number of Fock states (Sec. III). We then give detailed results of the H_2^+ photodissociation in Sec. IV and a summary and discussion in Sec. V.

II. THEORY

A detailed account of the theory is presented in Ref. [55]; here we only summarize the essential approach. The Schrödinger equation describing the time-dependent development of a molecule-photon system is given by

$$i\hbar\frac{\partial}{\partial t}\Phi_n(\mathbf{r},t) = (\hat{H}_M + n\hbar\omega)\Phi_n(\mathbf{r},t) + \frac{i}{2}E(t)\hat{\mu}[\Phi_{n-1}(\mathbf{r},t) - \Phi_{n+1}(\mathbf{r},t)]. \quad (1)$$

Where $\hat{H}_M$ is the molecular field-free Hamiltonian, describing M particles of charge q_m and three-dimensional vectors r_m, $m = 1,\ldots,M$, of x-direction dipole moment $\hat{\mu} = \sum_{m=1}^{M} q_m \hat{x}_m$, and

$$E(t) = \begin{cases} E_0 \sin^2\left(\frac{\pi}{\tau_p}t\right) & t \in [0,\tau_p] \\ 0 & \text{otherwise} \end{cases} \quad (2)$$

is the time-dependent electric field envelope pulse, assumed linearly polarized in the x direction, and E_0 is the pulse amplitude and τ_P its duration. ω is the photon frequency. The underlying molecular-photon wave function is assumed to be

$$\Psi(t) = \sum_n \Phi_n(\mathbf{r},t)|n\rangle, \quad (3)$$

where $|n\rangle$ is the Fock state of the light describing exactly $\bar{N}+n$ photons, and $\bar{N}$ is the average number of photons related to E_0 by [41]

$$\frac{1}{2}E_0 = \mathcal{E}_0\sqrt{\bar{N}}. \quad (4)$$

In Eq. (4), $\mathcal{E}_0 = \sqrt{\frac{\hbar\omega}{2\varepsilon_o\Omega}}$, where Ω is the volume of the cavity and ε_0 is the permittivity of the vacuum. We further assume that at $t = 0$, the initial state is a matter-light *product state*:

$$\Psi(t=0) = \Phi_{\rm int}(\mathbf{r}) \sum_n \gamma_n |n\rangle, \tag{5}$$

where γ_n are complex superposition coefficients defining the initial quantum state of the light. We will consider below two cases for the set γ_n. First, a standard coherent state laser source, in which the light state is a superposition of different photon-number states, with γ_n of Eq. (5) given by

$$\gamma_n = e^{-\frac{1}{2}|\alpha|^2} \frac{\alpha^{\bar{N}+n}}{\sqrt{(\bar{N}+n)!}} \qquad \alpha = \sqrt{\bar{N}} e^{i\theta}, \tag{6}$$

where θ is a constant phase. With this choice of initial wave function, $\Psi(t)$ remains at all times a matter-light product state (no entanglement), and the matter wave function obeys the "semiclassical" time-dependent Schrödinger equation (see Ref. [55])

$$i\hbar \frac{\partial}{\partial t} \Phi(\mathbf{r}, t) = [\hat{H}_M + E(t)\hat{\mu} \sin(\omega t - \theta)] \Phi(\mathbf{r}, t) \tag{7}$$

with $\Phi(\mathbf{r}, t=0) = \Phi_{\rm ini}(\mathbf{r})$. If the initial light state is not coherent, the light-matter state does not remain a product state, and entanglement quickly develops. Such will be the second case we consider, the canonical conjugate of a coherent state, namely, the "Fock state," characterized by a sharp photon number:

$$\gamma_n = \delta_{n,0}. \tag{8}$$

In Ref. [55], we showed that within the Born-Oppenheimer treatment, neglecting non-adiabatic couplings, one can obtain a "nuclear Schrödinger equation." For the coherent state case, this is the familiar equation

$$i\hbar \frac{\partial}{\partial t} \tilde{\phi}_j(\mathbf{R}, t) = [\hat{T}_N + u_j(\mathbf{R})] \tilde{\phi}_j(\mathbf{R}, t) + \bar{V}_{jj'}(t) \sin(\omega t - \theta) \tilde{\phi}_{j'}(\mathbf{R}, t), \tag{9}$$

with $\bar{V}_{jj'}(\mathbf{R}, t) = E(t)\hat{\mu}_{jj'}(\mathbf{R})$ and

$$\mu_{jj'}(\mathbf{R}) = \int \zeta_j(\mathbf{R}, \mathbf{s})^\dagger \mu_e(\mathbf{s}) \zeta_{j'}(\mathbf{R}, \mathbf{s})\, d^3\mathbf{s} + \delta_{jj'} \mu_N(\mathbf{R}) \tag{10}$$

are the total dipole moment electronic matrix elements, with $\hat{\mu}_e$ and $\hat{\mu}_N$ the electronic and nuclear dipole moment operators, respectively, and $\zeta_j(\mathbf{R}, \mathbf{s})$ are the electronic (adiabatic) eigenfunctions at position $\mathbf{R}$ of the nuclei and $u_j(\mathbf{R})$ are the adiabatic potential surfaces.

In the Fock state, a similar Born-Oppenheimer treatment would give (details are provided in Ref. [55])

$$i\hbar \frac{\partial}{\partial t} \psi_{nj}(\mathbf{R}, t) = [\hat{T}_N + u_j(\mathbf{R}) - n\hbar\omega] \psi_{nj}(\mathbf{R}, t) + [V_{jj'}(\mathbf{R}, t) \psi_{n-1,j'}(\mathbf{R}, t) + V^*_{jj'}(\mathbf{R}, t) \psi_{n+1,j'}(\mathbf{R}, t)]. \tag{11}$$

Here, and in Eq. (9) a summation over the repeated index j' is implied (Einstein's convention), $V_{jj'} = \frac{i}{2} E(t) \hat{\mu}_{jj'}(\mathbf{R})$.

TABLE I. Parameters of the photodissociation EM pulse.

Parameter	Symbol	Eq.	Value
Photon energy	$\hbar\omega$	(1)	1.57 eV
Maximal Electric field	E_0	(2)	$0.038 E_h\ (e\ a_0)^{-1}$
Pulse duration	τ_p	(2)	10, 20, 45 fs
Power flux			50 TW cm^{-2}
Photon wavelength			790 nm
Polarization			Linear along molecular axis

III. APPLICATION: PHOTODISSOCIATION OF H_2^+

In this section, we discuss application of the formalism to the photodissociation of H_2^+, where the products are a proton and a ground-state hydrogen atom. We summarize the pulse parameters in Table I.

We assume alignment of the H_2^+ molecular axis with the direction of light polarization and treat dynamically only the internuclear distance R. As we are interested in photoproducts at their ground states, we limit our study to the two basic adiabatic potential curves $u_0(R)$ and $u_1(R)$ corresponding to the bonding $1\sigma_g$ and antibonding $1\sigma_u$ states, shown as full line curves in Fig. 1. We have also performed a few pilot runs referring to an additional four excited states of H_2^+. We found that the presence of these states did not significantly affect the results.

The adiabatic surfaces and transition dipole moments μ_{01} for this calculation were obtained from *ab initio* calculations employing the 6-311++$G(3df, 3pd)$ basis set using the Hartree-Fock option of MOLPRO [56]. The calculated potentials compare well with the analytical results of Ref. [57]. They are depicted in Fig. 1. At large internuclear distance R, the two curves coalesce as they both describe a proton and a H atom in its ground state. The H_2^+ is assumed to be initially in the vth ($v = 0, 1, 2, \ldots$) vibrational eigenstate of $u_0(R)$. The difference $u_1(R_0) - u_0(R_0)$, where R_0 is the minimum

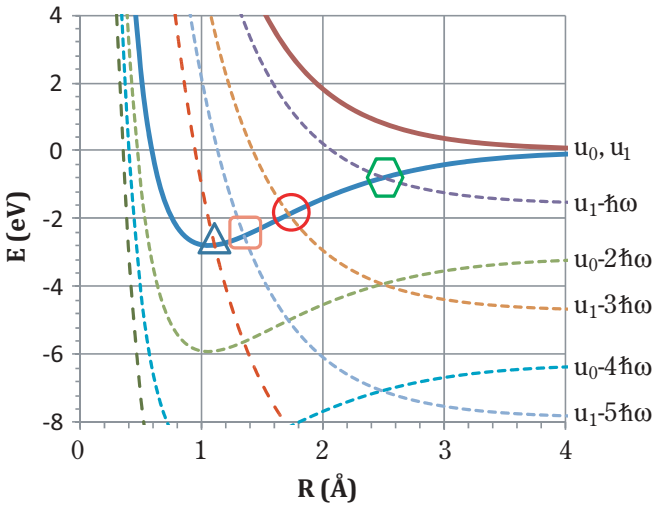

FIG. 1. (Color online) The full lines correspond to the ground $u_0(R)$ and the excited $u_1(R)$ adiabatic potentials. The dashed lines are first potentials on the diagonal of the potentials matrix $W(R)$ of Eq. (14) formed from photon-displaced adiabatic potentials u_0 and u_1.

of $u_0(R)$, is much larger than the photon energy ($\hbar\omega \sim 2.1$ eV), so photodissociation via transitions into the dissociative surface is efficient only for intense pulses.

A. Simplification of the equations

The index n can be either positive (emission of photons) or negative (absorption of photons); we only treat negative values of n. We neglect the possibility of total stimulated emission, i.e., we neglect the case where n is positive. This assumption is fully justified for $v < 7$. For $v > 7$, the emission is still negligible, since $u_1 - u_0$ is very large when the nuclear separation R is small.

The coupling matrix $V_{jj'}$ has only nondiagonal elements. The state ψ_{00} will thus couple only to $\psi_{-1,1}$. Similarly, ψ_{-11} will couple to ψ_{00} and to ψ_{-20}. Further consideration shows that ψ_{-20} couples to ψ_{-11} and ψ_{-31}. The emerging pattern is $\psi_{-n,j}$ couples to $\psi_{-n'j'}$ only if $j-n$ and $j'-n'$ are both even or both odd. Thus, there are two uncoupled manifolds. Since our initial condition is the state ψ_{00}, the "odd" manifold is never occupied and can be discarded. Under these conditions, it is only necessary to consider the equation

$$i\hbar\frac{\partial}{\partial t}\Theta(R,t) = \hat{T}_N\Theta(R,t) + W(R,t)\Theta(R,t), \qquad (12)$$

where Θ is the "even" column vector given by

$$\Theta = (\,\psi_{0,0}\;\; \psi_{-1,1}\;\; \psi_{-2,0}\;\; \psi_{-3,1}\;\; \cdots)^T \qquad (13)$$

(note that in ψ_{nj} we consider only the negative values of n since we address only photon *absorption*, as discussed above), and $W_{jj'}(R,t)$ is given by

$$W = \begin{pmatrix} u_0 & V_{01} & & & & \\ V_{10}^* & u_1-\hbar\omega & V_{01} & & & \\ & V_{10}^* & u_0-2\hbar\omega & V_{01} & & \\ & & V_{10}^* & u_1-3\hbar\omega & V_{01} & \\ & & & V_{10}^* & \ddots & \ddots \\ & & & & \ddots & \ddots \end{pmatrix}. \qquad (14)$$

This simplifies the treatment of the equations. Note the interesting structure of the equations: for the system to be in the σ_g electronic state (u_0 potential), it must have absorbed an even (including zero) number of photons; while for it to be in the σ_u electronic state (u_1), it must have absorbed an odd number of them. We show several of the first potentials on the diagonal of the W matrix in Fig. 1. It is seen that the u_0 curve is intercepted by several (in principle infinite) $u_1 + n\hbar\omega$ curves, $n = -1, -3, -5, \ldots$. We denote the first interception by a hexagon. This interception is direct, since the u_0 and $u_1 - \hbar\omega$ curves are directly coupled by V_{01}. The next interception, denoted by a circle, is between the u_0 and $u_1 - 3\hbar\omega$ curves. These two curves are only indirectly coupled: u_0 is coupled to $u_1 - \hbar\omega$, which is coupled to $u_0 - 2\hbar\omega$, which finally couples to $u_1 - 3\hbar\omega$. This is a "second-order coupling." It is natural to assume that this coupling is weaker than the direct coupling, and we will see below that indeed this is the case. The next two interceptions are between u_0 and either $u_1 - 5\hbar\omega$ (denoted by a square) or $u_1 - 7\hbar\omega$ (denoted by a triangle). These intersections will describe even weaker interactions, since they are fourth- and sixth-order interactions. In the Fock-state calculation, the wave packet starts at time $t = 0$ on the u_0 surface. It is thus clear that only a small finite number of photonic states are required, because the coupling becomes smaller as the number of states grows. We shall see this is indeed so in the next section.

The time propagation method and the details of the kinetic energy distribution analysis were discussed in Ref. [55] and will not be repeated here. We mention that for the numerical calculation, we use a grid consisting of 4096 points spanning the range $0.3 < R < 12$ Å. We placed at the asymptote an absorbing potential, guaranteeing efficient absorption of the photodissociated amplitude before reflection off the grid boundaries [58–61]. We included in all calculations six photonic states (i.e., there were 12 electrophoton states altogether). The propagation of the vector-wave equation uses a combination of the fast Fourier transform (FFT) [62–64] and by the Lanczos short-time iteration techniques [65–69].

The kinetic energy (KE), or E_k, distribution as was determined from the amplitude of the time-dependent (TD) wave packets [55] is

$$K_{nj}(E_k|v_i,nj) = \sqrt{\frac{2E_k}{h^2\mu_H}}\left|\int_0^\infty \psi_{nj}(R_a,t'|v_i) \times e^{i(E_k-n\hbar\omega)t'/\hbar}\,dt'\right|^2, \qquad (15)$$

where the prefactor is the normalization constant, ensuring that the integral of K_{nj} over all values of the KE is equal to the total photodissociation probability

$$P_{nj}(t\to\infty|v_i) = \int_0^\infty K_{nj}(E_k|v_i,nj)\,dE_k. \qquad (16)$$

B. Adiabatic electrophotonic potentials

One basic question concerns the number of photon states, or electrophotonic potentials, that have to be included in the calculation. It is evident from the explicit form of the matrix W in Eq. (14) that as its dimension M increases, the high j diagonal terms $W_{j,j}$ become dominated by $-j\hbar\omega$, while the off-diagonal terms are independent of j but are proportional to the amplitude of the electric field envelope E_0. For the coupling to be ineffective, the diagonal term must be much larger than the coupling:

$$M\hbar\omega \gg E_0\mu_{01}. \qquad (17)$$

In the H_2^+ photodissociation considered here, the field intensity is $E_0 \approx 0.038$ a.u., corresponding to a pulse maximal intensity of 50 TW/cm^2, and the transition dipole moment is of the order of $1a_0\ e$. Thus, for a photon of 1.7 eV, we obtain that the number M must be larger than unity. We demonstrate this by comparing the calculated kinetic energy distribution of the proton in the H_2^+ photodissociation starting in the $v = 6$ vibrational state, using $M = 2$, 4, and 6 electrophotonic potentials, shown in Fig. 2. It is seen that the calculation using just $M = 2$ potentials is very different

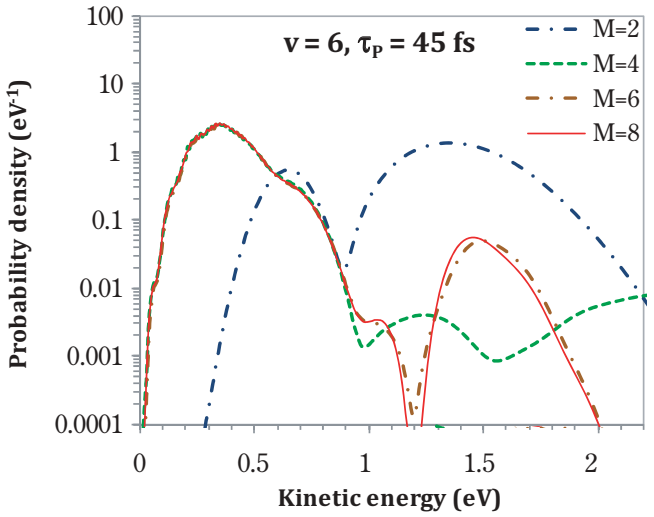

FIG. 2. (Color online) The total asymptotic KE distribution in H_2^+ photodissociation (internal vibrational state $v = 6$) photodissociation by a 45 fs Fock-state electromagnetic pulse calculated using $M = 2$, 4, 6 and 8 electro-photonic potentials.

from that using $M = 4$, while the latter is nearly identical with the $M = 6$ calculation for kinetic energies of up to 0.9eV. Comparing to $M = 8$, we see that beyond this energy range up to 2 eV, the $M = 6$ calculation is reasonably converged. We find then that the number of electrophotonic states needed to converge the calculation is sensitive to the kinetic energy of the photo fragments: a higher kinetic energy requires an increased number M of potentials. The calculations shown below all use $M = 6$ potentials and were checked for convergence.

Further insight can be gained by looking at the "adiabatic-dressed potentials," i.e., the potentials obtained by diagonalizing the potential matrix of Eq. (14). The results for maximal coupling (when the electric field attains its maximal value) are shown for $M = 2$, 4, 6, and 8 in Fig. 3. One can compare these potentials with the zero coupling (zero-field) potentials in Fig. 1. The strong field strongly distorts the shapes of the potentials, especially for large internuclear distances. This is a result of the linearly growing transition dipole moment for H_2^+ (equal, in atomic units, to $eR2$ at large R). Studying the patterns shown in Fig. 3, we first discuss the $M = 2$ panel. We number the dressed potential curves starting with #1 for the highest energy curve, #2 for the next to highest, etc. Dressed potential curves #1 and #2 are formed primarily by the mixing of the u_0 and $u_1 - \hbar\omega$ curves of Fig. 1. At small R, the curves have very different energies and do not interact significantly. Indeed the potential well of curve #2 is similar to that of u_0 in Fig. 1. At larger R, the u_0 and $u_1 - \hbar\omega$ curves approach, and they intersect $R \approx 2.5$ Å. The strong coupling by the field (in this study the coupling is $\sim \frac{R}{4a_0} eV$) forms a large avoided

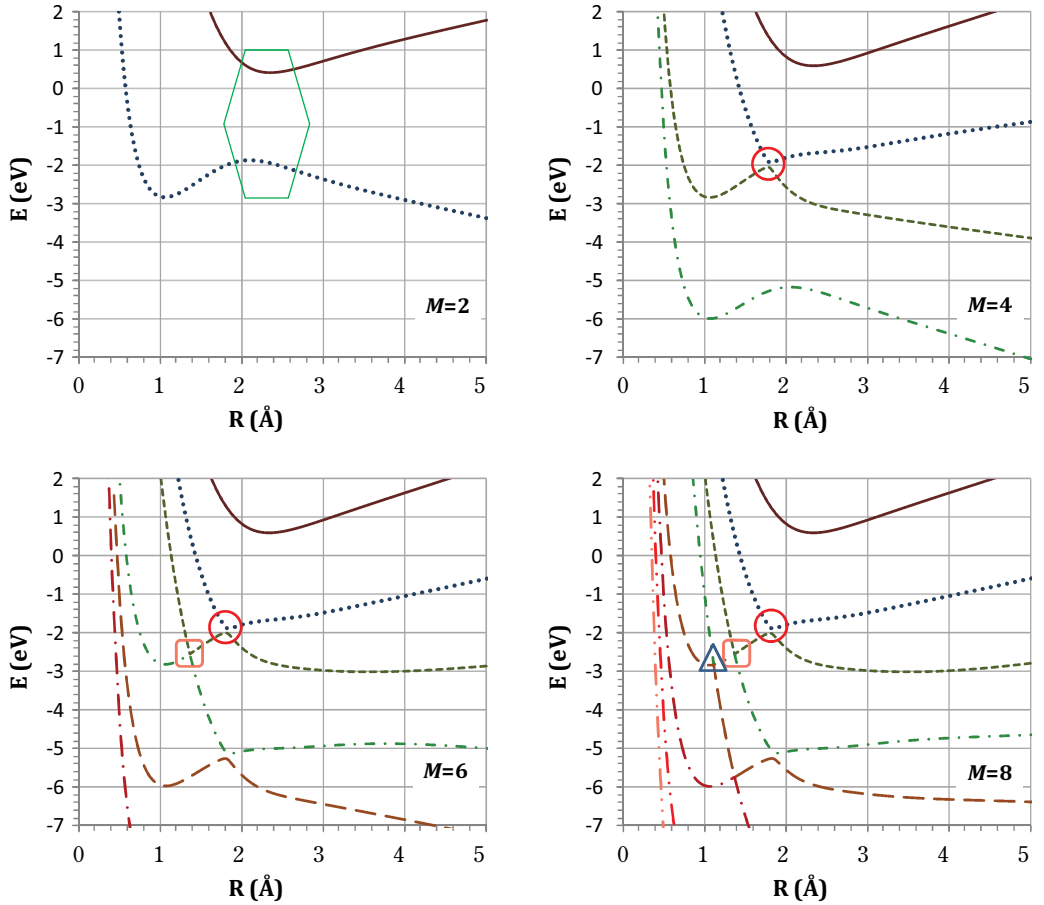

FIG. 3. (Color online) The adiabatic-dressed electrophotonic states at maximal electric field coupling E_0 (see Table I), with $M = 2$, 4, 6, and 8 states. Avoided crossing gaps: hexagon ≈2.5 eV, circle ≈0.1 eV, square ≈0.01 eV, and triangle ≈0.001 eV.

crossing gap, of more than ∼2 eV, in the dressed potential curves #1 and #2. This causes the formation of a barrier in curve #2 at $R \approx 2.2$ Å. When two additional states are added to the matrix, the picture changes dramatically. The curve resembling u_0 in Fig. 1 for small values of R is now curve #3. For larger values of R, it is very different from u_0 as it is further distorted by the interception of $u_1 - 3\hbar\omega$ with u_0. This causes an avoided crossing between curves #2 and #3 at $R \approx 1.9$ Å, denoted by a circle. This crossing exhibits a much smaller gap, of about 0.15 eV, a result of the fact that u_0 and $u_1 - \hbar\omega$ do not interact directly but through a second-order coupling discussed above. The small gap will cause strong nonadiabatic effects, the dynamics will bifurcate at this crossing, and both curves #2 and #3 will be important. It is therefore clear that the $M = 4$ and $M = 2$ dynamics will be very different. The next panel of $M = 6$ allows taking the crossing of u_0 with $u_1 - 5\hbar\omega$. This again causes a splitting of the curves, but the gap is now very small, only 0.01 eV. Thus only a small amount of wave packet will stay on curve #4, most will transfer to curve #3. The small amount staying on curve #2 will exhibit kinetic energy of ∼2 eV (the difference between the minimum of curve #2 and its asymptotic value). This is the reason why the calculation with $M = 6$ states is not converged for this kinetic energy range, as seen in Fig. 2. The $M = 8$ panel allows coupling of u_0 to an additional state ($u_1 - 7\hbar\omega$), but the coupling now is extremely weak (the gap is 0.001 eV) and does not significantly affect the dynamics unless kinetic energies around 4 eV are considered.

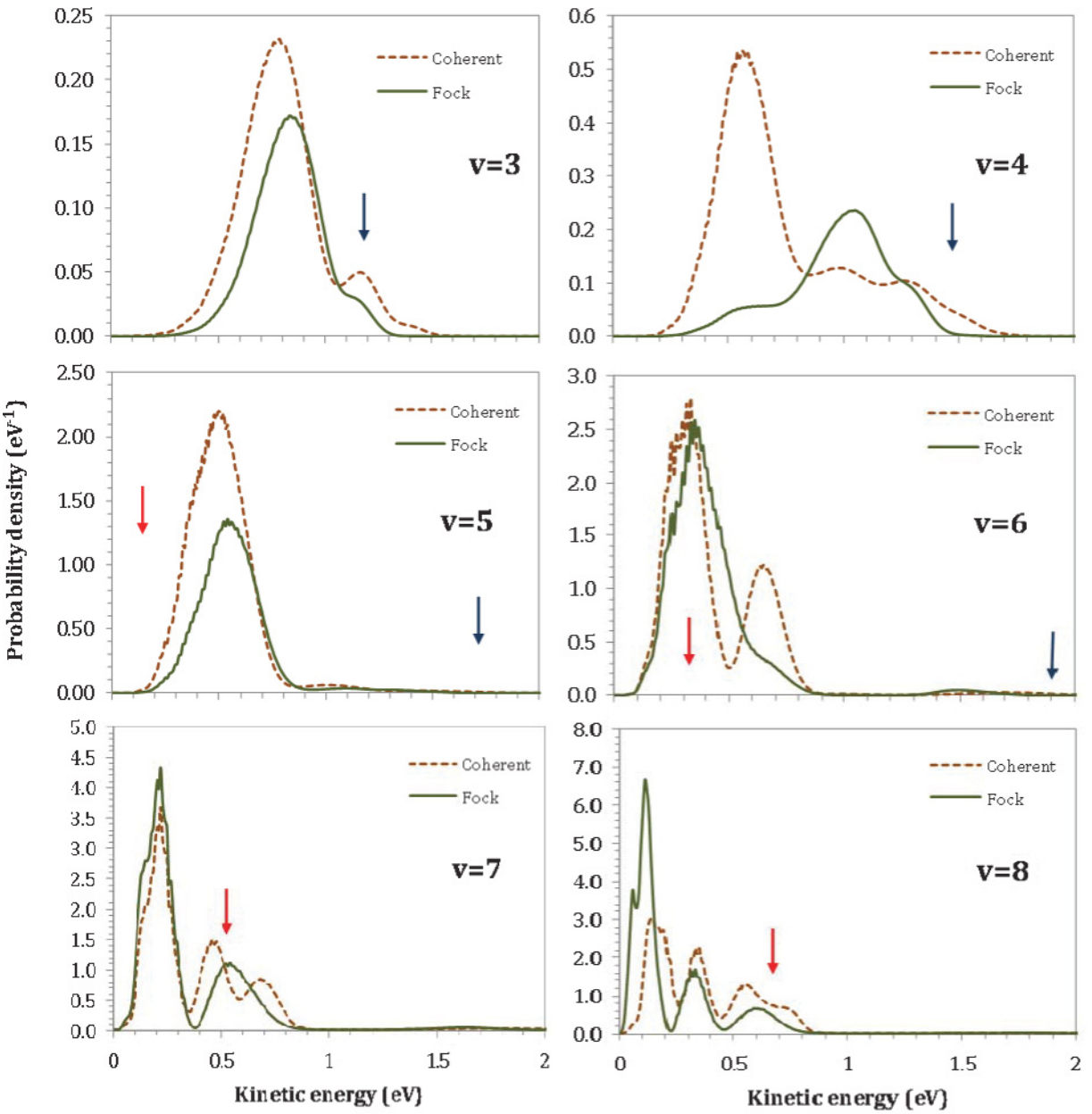

FIG. 4. (Color online) The total asymptotic KE distribution in H_2^+ photodissociation for 45 fs pulses when the initial molecular state is a sharp vibrational state ($v = 3$–8) and the electromagnetic field is in a coherent or a Fock state. Red (blue) arrow is the kinetic energy corresponding to absorption of a one (two) photon(s). Pulse parameters are given in Table I.

IV. RESULTS FOR PHOTODISSOCIATION OF H_2^+

In the specific calculation made here, we used $R_a = 6$ Å and then repeated the calculation with $R_a = 12$ Å checking that results are converged for this parameter. The kinetic energy distribution up to 3 eV was almost unaffected by the two choices. For higher kinetic energies, there was a difference. A component with kinetic energy E_k arrives at the asymptote R_a within time $R_a\,(2E_k/\mu_H)^{-1/2}$. The kinetic energy measurement at R_a [i.e., Eq. (15)] is only valid if the coupling between the surfaces is already zero by then. Thus, we estimate $R_a > \tau_p\,(2E_k/\mu_H)^{1/2}$ for the kinetic energy distribution at E_k to be valid. In practice, we noticed that this happens even sooner (probably even if R_a is smaller by a factor of 2, this still holds), and we conclude that measuring kinetic energy distributions up to 3 eV with $R_a = 12$ Å gives reasonably converged results.

A. Kinetic energy distribution

The initial state is an eigenstate of the unperturbed Hamiltonian, so naively the KE distribution is expected to reflect energy conservation rules, that is,

$$E_k(n, v) = \hbar\omega n + [u_0(R_0) + E_v] - u_0(\infty), \qquad (18)$$

where the quantum number n indicates the number of photons absorbed and E_v is the energy of the initial vibrational state. Equation (18) holds for an infinite duration [the so-called continuous wave (CW)] pulse. In our calculations, the pulse is turned on and off within 45 fs. This switching may lead to large deviations from Eq. (18), and we shall see that the coherent and Fock-state pulses differ significantly in this aspect. The KE distribution of the proton in the H_2^+ photodissociation as calculated for a 45 fs pulse assuming an initial coherent and Fock electromagnetic field is shown in Fig. 4 (for $v = 3$–8)

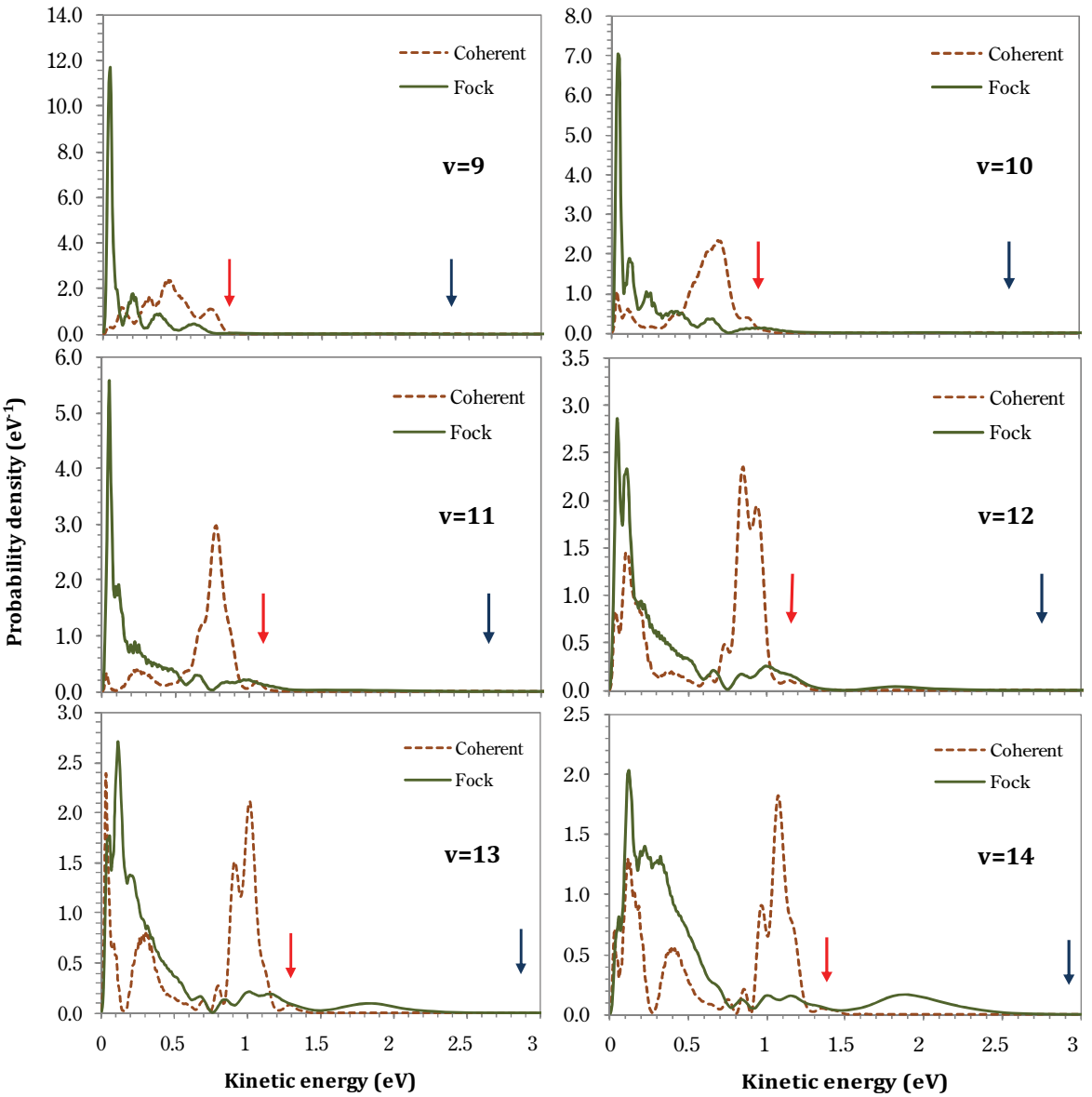

FIG. 5. (Color online) The total asymptotic KE distribution in H_2^+ photodissociation for 45 fs pulses when the initial molecular state is a sharp vibrational state ($v = 9$–14), and the electromagnetic field is in a coherent or a Fock state. Red (blue) arrow is the kinetic energy corresponding to absorption of a one (two) photon(s). Pulse parameters are given in Table I.

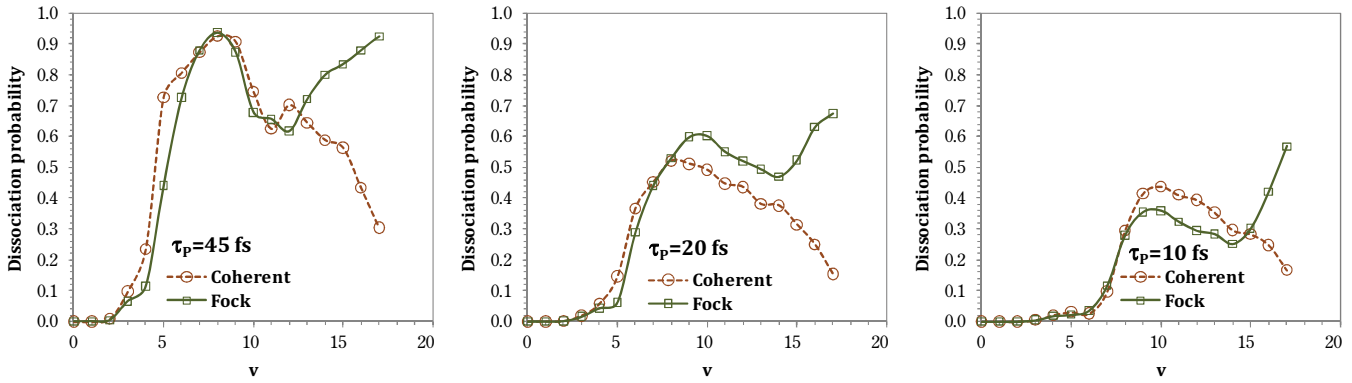

FIG. 6. (Color online) The dissociation probability as a function of the initial vibrational state of H_2^+ for three pulse durations. Pulse parameters are given in Table I.

and Fig. 5 ($v = 9$–14). It is seen that the shape of the KE distribution is strongly dependent on the initial vibrational state and electromagnetic state (whether coherent or Fock). The $v = 3, 4$ spectra exhibit relatively high kinetic energy peaks similar those expected for two-photon absorption (blue arrow). For $v > 4$, the KE is similar to that obtained after absorbing a single photon. Except for $v = 4$, the KE distribution for $v = 3$–8 of the coherent and Fock-state pulses are fairly similar, although the details are different. The vibrational energy of the $v = 4$ state is slightly above the adiabatic barrier (indicated by the red circle in Fig. 3, plate $M = 6$ or 8). This fact makes the dynamics of the photodissociation sensitive to all details of the calculation, because of the large role of tunneling and interference effects in this threshold case. This may explain the large difference between the photodissociation spectra caused by the coherent and Fock-state pulses in this case. Starting with $v = 9$ and up the KE distribution caused by the coherent-state pulse becomes very different from that of the Fock-state pulse. The coherent-state distribution seems to behave more like the CW case, with KE peaks close to the position of the red arrows. On the other hand, that caused by the Fock-state pulse is strongly biased toward low KEs. Near-zero KE releases were observed experimentally (using coherent-state pulses, of course) using 266 nm photons [70] and this phenomenon, for high vibrational states, was explained based on the dressed potential bond hardening arguments [70,71]. Here we find that for high vibrational states, the near-zero KE is considerably enhanced when the light is in a Fock state. Another evident difference between the coherent and Fock-state KE distributions is the development in the latter case of a high KE peak (at 1.5–2 eV) for initial vibrational states with $v > 13$.

B. Vibrational resolved dissociation probability

In the left panel of Fig. 6, we show the total dissociation probability as a function of the initial vibrational state for the coherent and Fock states of the EM field. The photodissociation is maximal at $v = 9$ for both the Fock and coherent field. However, as v is increased, the two light fields produce a different qualitative behavior. As v increases, the photodissociation probability by the coherent pulse drops, a known effect called "stabilization" or "vibrational trapping" [15,72]. The Fock pulse also exhibits reduction in photodissociation probability as v is increased from $v = 10$ up to $v = 13$. Subsequently the probability *increases* toward unity. We have also repeated such calculations for shorter pulse durations of 20 and 10 fs (center and right panels of Fig. 6) resulting in a similar behavior. It is somewhat surprising that the Fock states do not produce the stabilization effect, since that phenomenon has been explained qualitatively in terms of trapped vibrational states in the same Floquet dressed potentials as we used [14,15,72].

C. Pump-probe ionization-photodissociation of H_2

So far, we have mainly studied the photodissociation from a given vibrational state of H_2^+. One experimentally important observable is the photodissociation resulting from a two-pulse setup, in which a short pump pulse hits a H_2 molecule and ionizes it "suddenly" followed after a time delay τ_D by a probe pulse hitting the molecular ion and causing photodissociation. We use the results calculated here to estimate the kinetic energy distribution within the Franck-Condon approximation, where we assume that the first pulse creates a wave packet on the cation potential curve given by

$$\phi(t=0) = \psi_{v=0}^{H_2} = \sum_v e^{-iE_v\tau_D/\hbar}\phi_v\langle\phi_v|\phi_{v=0}^{H_2}\rangle, \qquad (19)$$

where $\langle\phi_v|\phi_{v=0}^{H_2}\rangle$, $v = 1, 2, 3, \ldots$, are the Franck-Condon (FC) factors, E_v is the vibrational energy of H_2^+, and $\psi_{v=0}^{H_2}$ is the vibrational ground-state wave packet of the electronic ground-state potential of H_2. Using this wave function as the initial wave packet allows the estimation of the KE distribution in pump-probe photodissociation of H_2. In Fig. 7, we show the KE distributions for three pump-probe delay times $\tau_D = 0$, 10, and 20 fs and the three pulse widths $\tau_P = 10$, 20, and 45 fs. One striking effect is the large sensitivity of the KE distribution to the pulse durations and the delay times. We find that as the pulse duration decreases, the total probabilities are generally reduced, but high kinetic energies are more probable than in the longer pulses. In terms of total probability, there is not a large difference between the coherent and Fock-state probe pulses, usually the former shows higher probability by 10–20%. A

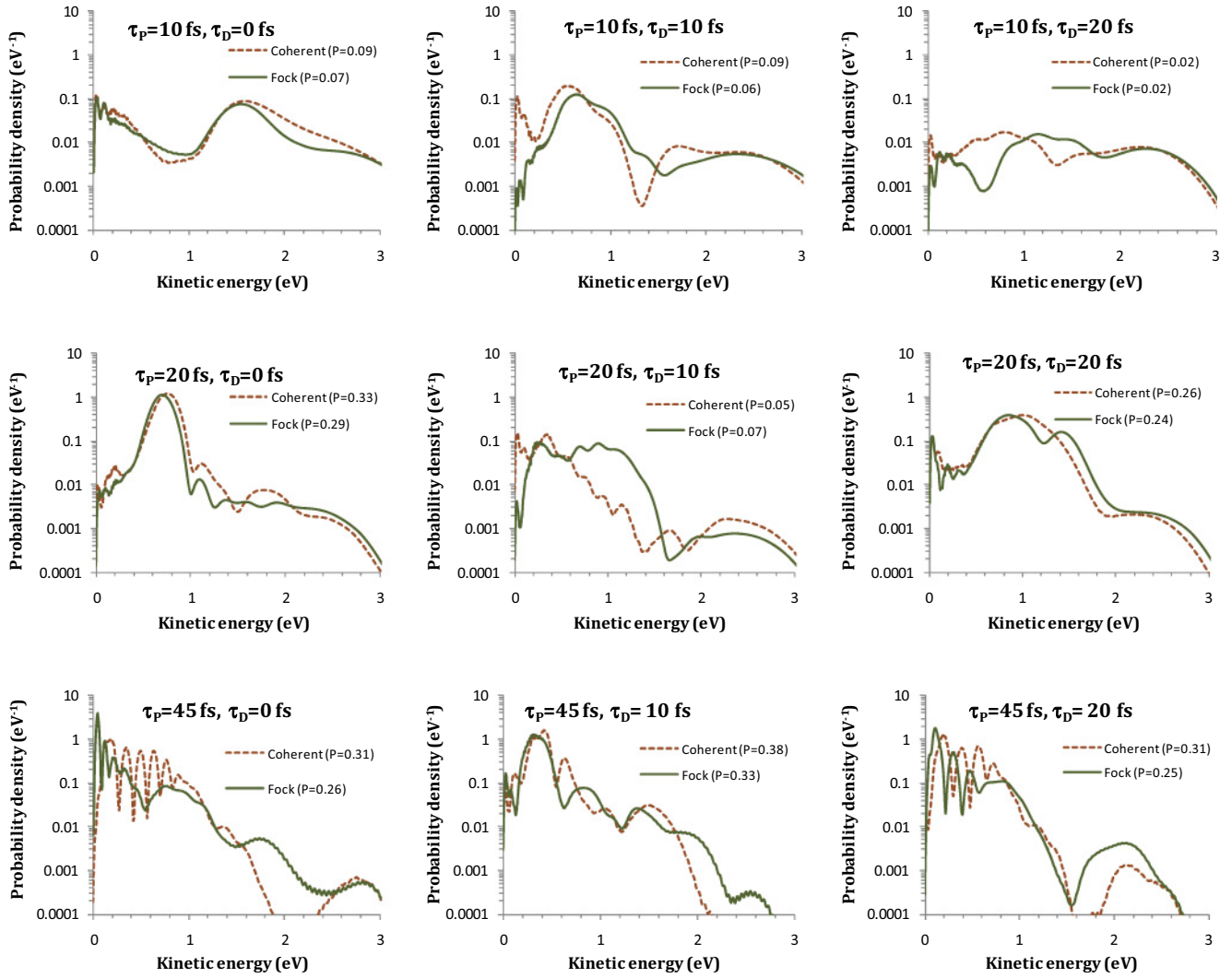

FIG. 7. (Color online) The total asymptotic KE distributions in H_2 pump-probe photodissociation using probe pulses of pulse duration τ_P = 10, 20, and 45 fs with pump-probe delay time of τ_D = 0, 10, and 20 fs. The legend indicates the total photodissociation probability P. It is assumed that the initial molecular state is the ground $v = 0$ H_2 vibrational wave packet (Franck-Condon approximation).

large difference is seen when we compare the KE distributions. The Fock-state probe is often (but not always) more efficient at producing the higher kinetic energy dissociations.

V. SUMMARY AND DISCUSSION

We have presented a study of H_2^+ photodissociation where the initial quantum state of light is a Fock state, comparing results to conventional coherent-state pulses of similar characteristics. The equations of motion include a coupling of the molecular Hamiltonian to several Fock states of the oscillator representing the radiation field. We found that only a small number ($M = 6$) of photonic (harmonic oscillator) states are needed in order to converge the photodissociation dynamics of the H_2^+ system, in the kinetic energy range of up to 3 eV. We explained this finding in terms of the diabatic coupling hierarchies. For both coherent and Fock-state pulses, the kinetic energy distribution was sensitive to the initial vibrational state of H_2^+. In some cases, especially for the threshold vibrational states (around $v = 4$) and for large vibrational quanta, there was a significant sensitivity of the KE distribution to the quantum state of the electromagnetic field.

Our finding, that certain aspects of the photodissociation molecular dynamics are sensitive to the quantum state of light, implies that photochemistry may gain from the emerging quantum light technology [44,54,73]. The results may also be useful as a sort of "stability analysis": the effect of Fock perturbations of the coherent state [51] in the photodissociation dynamics.

ACKNOWLEDGMENTS

This work was supported by the Binational USA-Israel Science Foundation. S.A. acknowledges support by the Department of Science and Technology (DST, Government of India) through Project No. SR/S1/PC/13/2008.

[1] M. Gavrila *Atoms in Intense Laser Fields* (Academic Press, San Diego, 1992).

[2] P. B. Corkum *et al.*, Faraday Discuss. **113** (113), 47 (1999).

[3] C. N. Cohen-Tannoudji, Rev. Mod. Phys. **70**, 707 (1998).

[4] M. Drescher *et al.*, Science **291**, 1923 (2001).

[5] R. Kosloff, S. A. Rice, P. Gaspard, S. Tersigni, and D. J. Tannor, Chem. Phys. **139**, 201 (1989).

[6] A. H. Zewail *et al.*, in *Chemical Reactions and Their Control on the Femtosecond Time Scale: XXth Solvay Conference on Chemistry*, edited by P. Gaspard and I. Burghardt (Wiley, New York, 1997), p. 3.

[7] S. A. Rice, Nature (London) **403**, 496 (2000).

[8] G. G. Balint-Kurti, F. R. Manby, Q. H. Ren, M. Artamonov, T. S. Ho, and H. Rabitz, J. Chem. Phys. **122**, 084110 (2005).

[9] R. deVivieRiedle *et al.*, J. Phys. Chem. **100**, 7789 (1996).

[10] H. Niikura, F. Legare, R. Hasbani, M. Y. Ivanov, D. M. Villeneuve, and P. B. Corkum, Nature (London) **421**, 826 (2003).

[11] F. Krausz, Phys. World **14**(9), 41 (2001).

[12] P. H. Bucksbaum, Nature (London) **421**, 593 (2003).

[13] P. H. Bucksbaum, A. Zavriyev, H. G. Muller, and D. W. Schumacher, Phys. Rev. Lett. **64**, 1883 (1990).

[14] F. H. Mies, A. Giustisuzor, K. C. Kulander, and K. J. Schafer, Super Intense Laser-Atom Physics **316**, 329 (1993).

[15] A. Zavriyev, P. H. Bucksbaum, J. Squier, and F. Saline, Phys. Rev. Lett. **70**, 1077 (1993).

[16] K. C. Kulander, F. H. Mies, and K. J. Schafer, Phys. Rev. A **53**, 2562 (1996).

[17] A. Assion, T. Baumert, J. Helbing, V. Seyfried, and G. Gerber, Phys. Rev. A **55**, 1899 (1997).

[18] S. M. Hankin, D. M. Villeneuve, P. B. Corkum, and D. M. Rayner, Phys. Rev. A **64**, 013405 (2001).

[19] A. Palacios, H. Bachau, and F. Martin, J. Phys. B **38**, L99 (2005).

[20] M. F. Kling *et al.*, Science **312**, 246 (2006).

[21] T. Ergler, A. Rudenko, B. Feuerstein, K. Zrost, C. D. Schroter, R. Moshammer, and J. Ullrich, Phys. Rev. Lett. **97**, 193001 (2006).

[22] B. D. Esry, A. M. Sayler, P. Q. Wang, K. D. Carnes, and I. Ben-Itzhak, Phys. Rev. Lett. **97**, 013003 (2006).

[23] J. McKenna *et al.*, Phys. Rev. Lett. **100**, 133001 (2008).

[24] M. Baer and I. H. Zimmerman, in *Theory of Chemical Reaction Dynamics*, edited by M. Baer (CRC, Boca Raton, FL, 1985), Vol. 2, p. 265.

[25] I. Last and M. Baer, J. Chem. Phys. **82**, 4954 (1985).

[26] I. Last, M. Baer, I. H. Zimmerman, and T. F. George, Chem. Phys. Lett. **101**, 163 (1983).

[27] I. H. Zimmerman, M. Baer, and T. F. George, J. Phys. Chem. **87**, 1478 (1983).

[28] S. Chelkowski, T. Zuo, and A. D. Bandrauk, Phys. Rev. A **46**, R5342 (1992).

[29] I. Last and J. Jortner, J. Chem. Phys. **121**, 3030 (2004).

[30] S. I. Chu and D. A. Telnov, Phys. Rep. **390**, 1 (2004).

[31] J. H. Posthumus, Rep. Prog. Phys. **67**, 623 (2004).

[32] E. Livshits and R. Baer, J. Phys. Chem. A **110**, 8443 (2006).

[33] H. A. Leth, L. B. Madsen, and J. F. McCann, Phys. Rev. A **76**, 033414 (2007).

[34] D. Barash, A. E. Orel, and R. Baer, Phys. Rev. A **61**, 013402 (1999).

[35] R. Baer, D. Neuhauser, P. R. Zdanska, and N. Moiseyev, Phys. Rev. A **68**, 043406 (2003).

[36] J. Manz, H. Naundorf, K. Yamashita, and Y. Zhao, J. Chem. Phys. **113**, 8969 (2000).

[37] I. H. Zimmerman, J. M. Yuan, and T. F. George, J. Chem. Phys. **66**, 2638 (1977).

[38] J. C. Light and A. Altenbergersiczek, J. Chem. Phys. **70**, 4108 (1979).

[39] A. D. Bandrauk and M. L. Sink, J. Chem. Phys. **74**, 1110 (1981).

[40] S. I. Chu, J. Chem. Phys. **75**, 2215 (1981).

[41] C. Cohen-Tannoudji, J. Dupont-Roc, and G. Grynberg, *Photons and Atoms: Introduction to Quantum Electrodynamics* (Wiley, New York, 1989).

[42] B. Dayan, Phys. Rev. A **76**, 043813 (2007).

[43] O. Roslyak and S. Mukamel, Phys. Rev. A **79**, 063409 (2009).

[44] M. Brune *et al.*, Phys. Rev. Lett. **101**, 240402 (2008).

[45] J. I. Cirac, R. Blatt, A. S. Parkins, and P. Zoller, Phys. Rev. Lett. **70**, 762 (1993).

[46] F. DeMartini, G. DiGiuseppe, and M. Marrocco, Phys. Rev. Lett. **76**, 900 (1996).

[47] A. I. Lvovsky, H. Hansen, T. Aichele, O. Benson, J. Mlynek, and S. Schiller, Phys. Rev. Lett. **87**, 050402 (2001).

[48] P. Bertet, S. Osnaghi, P. Milman, A. Auffeves, P. Maioli, M. Brune, J. M. Raimond, and S. Haroche, Phys. Rev. Lett. **88**, 143601 (2002).

[49] K. Sanaka, K. J. Resch, and A. Zeilinger, Phys. Rev. Lett. **96**, 083601 (2006).

[50] A. Ourjoumtsev, R. Tualle-Brouri, and P. Grangier, Phys. Rev. Lett. **96**, 213601 (2006).

[51] A. Zavatta, S. Viciani, and M. Bellini, Science **306**, 660 (2004).

[52] M. Bellini, A. Zavatta, and S. Viciani, in *The Nature of Light: What is a Photon?*, edited by Chandra Roychoudhuri, A. F. Kracklauer, and Kathy Creath (CRC, Boca Raton, FL, 2008), p. 278.

[53] G. Breitenbach, S. Schiller, and J. Mlynek, Nature (London) **387**, 471 (1997).

[54] A. I. Lvovsky and M. G. Raymer, Rev. Mod. Phys. **81**, 299 (2009).

[55] A. K. Paul *et al.*, J. Phys. Chem. A **113**, 7331 (2009).

[56] H.-J. Werner *et al.*, MOLPRO, a package of *ab initio* programs, 2006.

[57] D. R. Bates, K. Ledsham, and A. L. Stewart, Philos. Trans. R. Soc. London. Ser. A **246**, 215 (1953).

[58] D. Neuhasuer and M. Baer, J. Chem. Phys. **90**, 4351 (1989).

[59] G. J. Halasz and A. Vibok, Chem. Phys. Lett. **323**, 287 (2000).

[60] M. H. Beck, A. Jackle, G. A. Worth, and H. D. Meyer, Phys. Rep. **324**, 1 (2000).

[61] J. G. Muga, J. P. Palao, B. Navarro, and I. L. Egusquiza, Phys. Rep. **395**, 357 (2004).

[62] R. Kosloff and D. Kosloff, J. Chem. Phys. **79**, 1823 (1983).

[63] H. Tal-Ezer and R. Kosloff, J. Chem. Phys. **81**, 3967 (1984).
[64] R. Kosloff, J. Phys. Chem. **92**, 2087 (1988).
[65] J. K. Cullum and R. A. Willoughby, *Lanczos Algorithms for Large Symmetric Eigenvalue Computations* (Birkhauser, Boston, 1985).
[66] S. Adhikari, Chem. Phys. Lett. **262**, 526 (1996).
[67] P. Sarkar and S. Adhikari, Chem. Phys. Lett. **277**, 284 (1997).
[68] S. Adhikari, Chem. Phys. **226**, 25 (1998).
[69] A. Saha, P. Sarkar, and S. Adhikari, Int. J. Quantum Chem. **107**, 1285 (2007).
[70] J. H. Posthumus *et al.*, J. Phys. B **33**, L563 (2000).
[71] A. Giusti-Suzor and F. H. Mies, Phys. Rev. Lett. **68**, 3869 (1992).
[72] G. H. Yao and Shih I. Chu, Phys. Rev. A **48**, 485 (1993).
[73] H. Wang *et al.*, Phys. Rev. Lett. **101**, 240401 (2008).